EVLA Memo #127
On the Use of Correlation Coefficients for Determining Antenna Sensitivity

Rick Perley

August 21, 2008

Abstract

A simple method is developed to estimate antenna sensitivities through analysis of the array corrrelation coefficients. The accuracy of this method is demonstrated by comparison of the observed cold-sky noise with predictions based on this analysis applied to observations of 3C147. For nearly all cases, the predictions are within 2% of the observed values.

1 Introduction

The EVLA Project has set requirements for the antenna sensitivity expressed in terms of the System Equivalent Flux Density. This metric, denoted S_E, is defined as the spectral flux density of an external source which doubles the system temperature, and is thus a function both of the antenna's effective collecting area and of its system temperature. Determining the S_E of an antenna by directly measuring the system temperature and antenna efficiency is time consuming, requiring on-antenna calibration with hot and cold loads combined with observation of an external source of known flux density. For many applications, including monitoring system performance and estimating array sensitivity, it is not these individual characteristics that are needed, but rather their ratio, from which S_E can be directly determined. What is needed then is a simple and convenient method for determining this quantity.

Perley and Hayward, in EVLA Memo#119, outlined a simple method of determining the SEFD directly from analysis of the array correlation coefficients. However, they did not demonstrate that these derived quantities were in fact good measures of the actual sensitivity. In this memo, I review their method, extend the analysis to show how the derived SEFDs are related to array imaging sensitivity, and show that in fact these simply-derived measures are robust and accurate measures of antenna, and array, performance.

2 Deriving the SEFD from Array Correlation Coefficients

This section is essentially a repeat of the corresponding section in EVLA Memo#119.

The correlation coefficient ρ_{ij} for a two-element interferometer observing an unresolved source can be written

$$\rho_{ij} = \frac{\sqrt{T_{Ai}T_{Aj}}}{\sqrt{(T_{Ai}+T_{Si})(T_{Aj}+T_{Sj})}} \tag{1}$$

where the subscripts (i,j) denote the two component antennas, $T_A = S\epsilon A_p/2k$ is the antenna temperature due to an unpolarized source of spectral flux density S, A_p is the physical collecting area of a component antenna, and T_S is the antenna system temperature, which includes all uncorrelated noise components, including the electronics, atmospheric emission, and ground spillover.

Equation (1) can be written as

$$\rho_{ij} = \frac{SA_p}{2k}\sqrt{\frac{\epsilon_i}{(1+r_i)T_{Si}}\frac{\epsilon_j}{(1+r_j)T_{Sj}}} = \frac{S}{\sqrt{(1+r_i)S_{Ei}(1+r_j)S_{Ej}}} \tag{2}$$

where ϵ is the antenna efficiency, k is Boltzmann's constant, $r = T_A/T_{sys}$ is the ratio of the antenna temperature to system temperature, and

$$S_E = \frac{2kT_S}{\epsilon A_P} \tag{3}$$

defines the System Equivalent Flux Density. Normally, both S and S_E are expressed in Janskys, and I shall adopt this convention subsequently.

In general, a real correlator does not directly provide the correlation coefficients, but rather an estimate r_{ij} which must be corrected for various scaling factors. For the VLA's correlator, Bryan Butler, in AIPS Memo 108, has shown the relation to be

$$\rho_{ij} = \frac{r_{ij}}{\eta_s \eta_q} = 4.83 \times 10^{-3} r_{ij}, \tag{4}$$

where the $\eta_s = 256$ arises from an internal scaling, and $\eta_q = 0.809$ is the quantization efficiency of the VLA's 3-level correlator [1].

From Equations 2 and 4 we can relate the observed raw correlation coefficient, r_{ij}, to the geometric mean of the component antennas' system equivalent flux densities as

$$r_{ij} = \frac{\eta_s \eta_q S}{\sqrt{S_{Ei} S_{Ej}}} \frac{1}{\sqrt{(1+r_i)(1+r_j)}} \tag{5}$$

where S is the spectral flux density of the observed source, expressed in units of Janskys. For most observing, the antenna temperature due to the source is very much less than the system temperature, so that $r \ll 1$, and the right-most factor in Eqn. 5 can be set to 1.0 with negligible error. However, as I will show below, the accuracy of the described method is sufficient that the 0.5K increase in system temperature from observing a modest calibrator decreases the sensitivity by a measureable amount. I thus retain this factor throughout.

An array like the EVLA comprises many antennas, and we wish to conveniently determine the individual antenna sensitivities. For an array of N antennas, we have $N(N-1)/2$ correlations, so for $N = 3$ we can directly invert the three correlations to recover the S_E. For $N > 3$, a least-squares analysis is appropriate. All interferometer calibration packages include this capability, providing an estimate, G, of the amplitude gain for each antenna which converts the observed correlation coefficients to the known flux density:

$$S = G_i G_j r_{ij}. \tag{6}$$

The derived gains are related to the desired system equivalent flux densities by

$$S_E = \frac{\eta_s \eta_q G^2}{1+r} = \frac{207.1 G^2}{1+r}. \tag{7}$$

where the numerical factor applies to the VLA correlator.

The system equivalent flux density is not a familiar parameter to many users, most of whom are more used to thinking of antenna performance in temperature terms. I thus define a temperature parameter, called the effective system temperature, which is defined as

$$T_{eff} = \frac{T_{sys}}{\epsilon} \tag{8}$$

and is related to the System Equivalent Flux Density as

$$T_{eff} = \frac{A_p S_E}{2k} = 0.178 S_E = \frac{36.86 G^2}{1+r} \tag{9}$$

where the numerical form on the RHS is appropriate for the VLA's 25-meter antennas.

As I am one of those more used to thinking in terms of system temperature, I have utilized the T_{eff} parameter in what follows. To convert to S_E, multiply by 5.62.

[1] The quantization correction is non-linear in general, but can be linearized in the limit of low correlation coefficient

3 Noise on an Interferometer

For an ideal analog interferometer comprising two antennas whose SEFDs are S_{Ei} and S_{Ej}, with square bandwidth $\Delta\nu$ and integration time Δt, the rms noise in both the real and imaginary parts of the complex visibility is

$$\sigma_S = \frac{\sqrt{S_{Ei}S_{Ej}}\sqrt{1+r_i+r_j+2r_ir_j}}{\sqrt{2\Delta\nu\Delta t}} \tag{10}$$

A real interferometer comprising these same antennas, but with non-square bandpasses and digital processing will always have a higher noise due to losses associated with the electronics. We can write the rms noise value for a real two-element interferometer as

$$\sigma_S = \frac{\sqrt{S_{Ei}S_{Ej}}\sqrt{1+r_i+r_j+2r_ir_j}}{\eta_c\sqrt{2\Delta\nu\Delta t}} \tag{11}$$

where η_c is a 'backend' system efficiency which accounts for all losses due to the digital processing, and does not include the antenna efficiency.

The loss factor η_c depends on a number of factors, including:

- Quantizer loss, which depends *both* upon the quantization scheme and the sampling rate.
- Effective bandwidth, which would include SNR losses associated with attenuation by bandpass filters, and
- Effective integration time, which would include losses associated with correlator or data transmission dead times.

For the VLA's correlator, the quantizer efficiency is 0.89 for the continuum mode, where (since 1997) we are effectively oversampling by a factor of two[2], and is 0.81 for the spectral line modes. For both line and continuum modes, there is an additional factor of 0.98 associated with data waveguide blanking (this applies also to the the EVLA antennas during transition observing). Finally, for the line modes, there is an additional loss factor which depends upon the bandwidth, due to the use of recirculator memory. The efficiencies associated with this are given in the Table 1:

Bandwidth (MHz)	BW Code	Recirc. Loss	η_c
50	0	1.00	0.79
25	1	.998	0.79
12.5	2	.996	0.79
6.25	3	.993	0.79
3.125	4	.985	0.78
1.563	5	.970	0.77
0.781	6	.686	0.42
0.195	8	.485	0.38
0.195	9	.343	0.27

Table 1: VLA correlator efficiencies for spectral line modes (from Ken Sowinski). Given are the efficiencies associated with use of recirculator memory, and the overall efficiency. There is some uncertainty with the values for the three narrowest bandwidths. For the continuum modes, the efficiency is 0.87 for all bandwidths.

We can, therefore, determine the antenna sensitivities in two ways: Use the observed correlation coefficients, or use the observed noise statistics. Of these, the former is much preferred, as the process is more direct, and does not depend upon system bandwidth or integration time. Both methods should give the same result, providing that the bandwidths and integration times are confidently known. In this memo, I determine the antenna sensitivites via the first method, and use them to predict the noise distributions, for comparison to actual calibrated data.

[2]See Durga Bagri's VLA Test Memos #206 and 210 for details

4 Measurements

To establish that these relations hold with good accuracy for a working interferometer, I observed the calibrator source 3C147 plus a blank field one degree to the north with the VLA at 8485 and 8435 MHz in various line and continuum modes on 27 and 28 July, 2008. The continuum mode data were taken with the minimum integration time of 0.417 seconds at (nominal) bandwidths of 50, 25, 12.5, 6.25, 3.125, 1.56, and 0.78 MHz. The spectral line mode data were taken in a single polarization mode (mode '1A') at 50, 25, and 12.5 MHz bandwidths with 1.67 second averaging. Data were also taken at 6.25 MHz BW in mode '1A' with 3.33 seconds averaging. This mode provides the maximum spectral resolution. The single frequency full polarization mode 'PA' was also utilized at 6.25 and 12.5 MHz bandwidth.

The flux density of 3C147 is 4.8 Jy, which provides an antenna temperature of 0.52K (using $\epsilon = 0.6$). The ratio r between antenna and system temperatures is thus 0.015, and this value has been used in determining the S_E values. Note that the determination of the observed sensitivity was based on blank field observations, for which $r = 0$.

The T_{eff} and S_E values were determined through calibration in AIPS. Because the EVLA and VLA have different bandpasses – which causes decorrelation of typically $\sim$ 10% on baselines linking EVLA with VLA antennas – the antenna-based sensitivity parameters were determined separately for each array following the procedure described in Section 2.

5 Results

5.1 Continuum Observations

The variation of the T_{eff} parameter, as a function of bandwidth, is shown in Fig. 1 for the EVLA and VLA antennas.

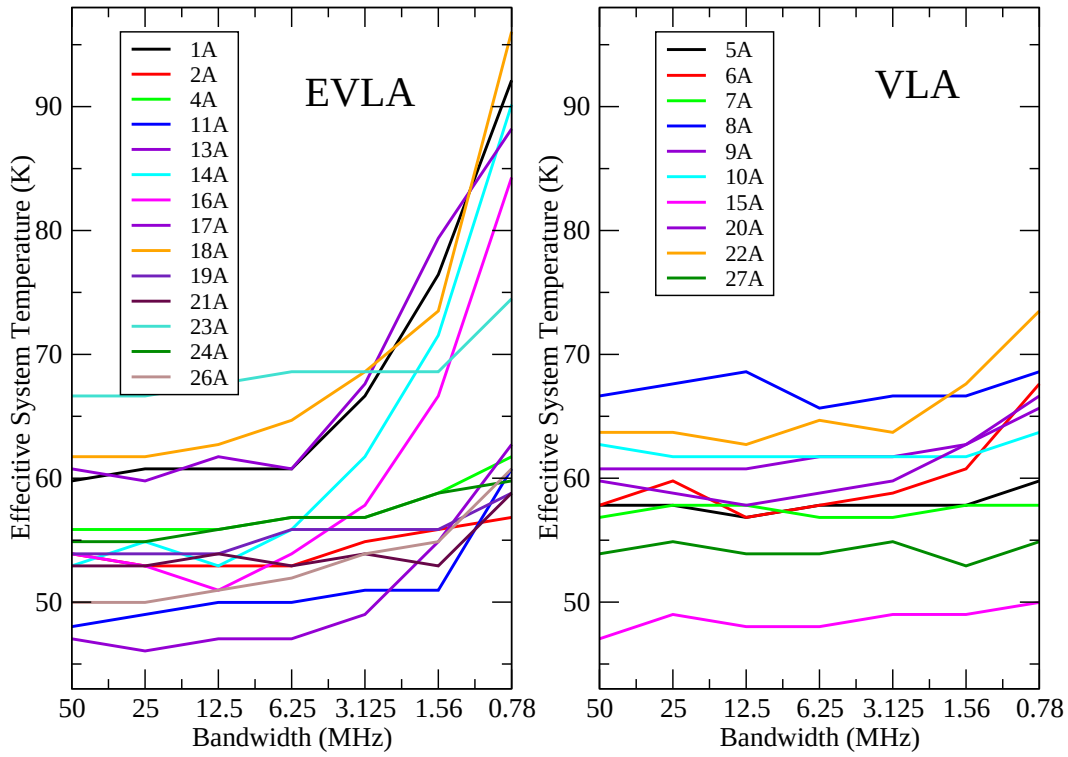

Figure 1: The effective system temperature, T_{sys}/ϵ, as a function of bandwidth for the EVLA (left) and VLA (right), for RCP in IF#1. The decline in sensitivity at narrow bandwidths for the EVLA antennas is due to aliasing in the transition filter. To obtain S_E, multiply by 5.62.

The figure shows that the EVLA and VLA antennas have nearly the same sensitivity – as expected since the

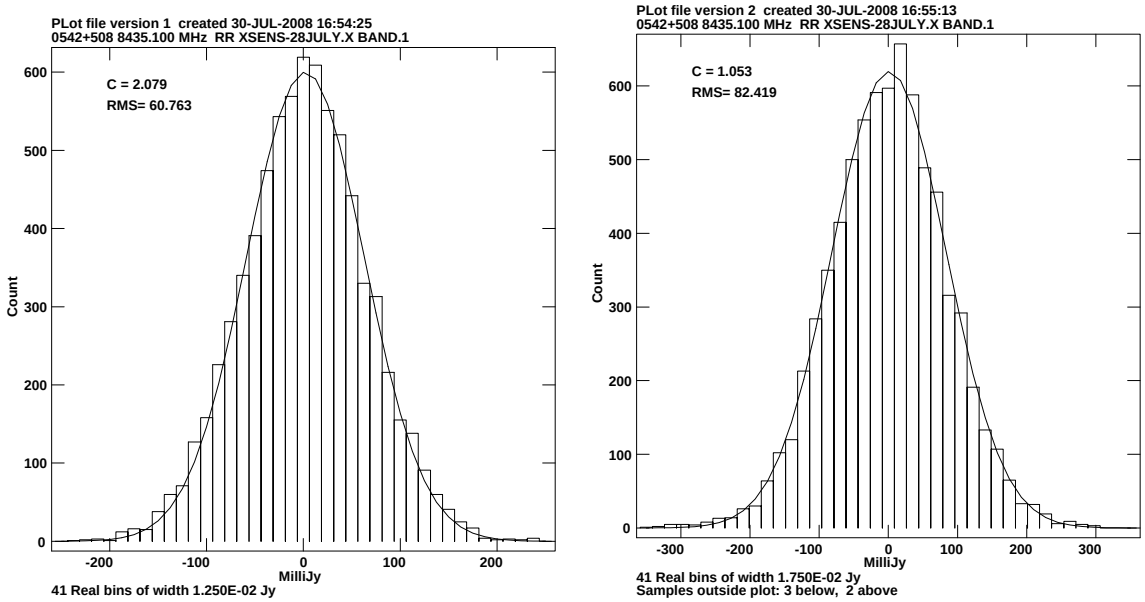

Figure 2: Noise histograms from the 10 most sensitive EVLA antennas, showing the distribution of the real part of the visibility from a blank field, in continuum mode. The left panel displays data from 50 MHz BW, the right panel shows the 25 MHz BW data. The averaging time was 417 milliseconds.

receivers are the same for both[3]. The best antennas show an effective system temperature of less than 50K – an excellent value which would be attained with a (real) system temperature of 30K, and an antenna efficiency of 0.60.

A notable feature of the EVLA antennas is a degradation of sensitivity for bandwidths less than 6.25 MHz. The origin of this is aliasing by the transition filter, which takes the EVLA's 8-bit digital sample stream, selects a 64-MHz-wide sub-band, and converts this to an analog signal which is then fed to the VLA correlator. See Revnell (EVLA Memo#97) for a description. This is a temporary problem which will disappear when the WIDAR correlator is operational.

The aliased emission is significant over the ∼500 kHz of the baseband end of the VLA's passband. What is not obvious is why the loss of correlation coefficient is so much stronger for some antennas (e.g., 14, 16, and 18), and much less notable for others (e.g. 2 and 26). A likely answer is that although the aliased receiver noise is the same for all antennas, the phase of the aliased source noise may vary from antenna to antenna. The resulting correlation coefficient will be very sensitive to the phase of the aliased signal.

The VLA antennas show almost no effect in their sensitivity upon bandwidth – as expected, since aliased noise is not expected to be significant. The small dependence noted can probably be attributed to bandpass attenuation.

If these derived values of S_E are correct, we should be able to predict the noise on a baseline when observing a blank field by using Equation 11, presuming we know the effective bandwidth and time integration of the system. The noise in a blank field was determined from observations of a field one degree north of the calibrator. In Fig. 2 I show typical noise histograms from these blank-field data, taken at 50 and 25 MHz bandwidth. The noise statistics were determined from both the real and imaginary parts of the visibility data for the ten most sensitive EVLA antennas (as determined from the correlation coefficients), and the eight most sensitive VLA antennas. These turn out to be very uniform in their antenna sensitivities, thus minimizing complications in weighting the statistics from antennas with disparate characteristics.

In Figure 3 I show the values of the observed noise (multiplied by $\sqrt{B_M}$, where B_M is the bandwidth in MHz) and the predictions made from the sensitivities derived from the correlation coefficients, using $\Delta t = 0.417$ seconds, $\eta_c = 0.87$, and the bandwidths at their nominal values. For these plots, only a subset of the antennas whose S_E values were similar were utilized. The agreement between predicted and observed sensitivity extremely good, except at the widest bandwidths, where it is clear that the effective bandwidth is much less than the nominal due to a very strong filter roll-off. If the loss of sensitivity is solely due to filter roll-off, the effective bandwidths

[3]The EVLA's new X-band receivers will not be implemented until after 2010. Until then, we are utilizing the existing systems.

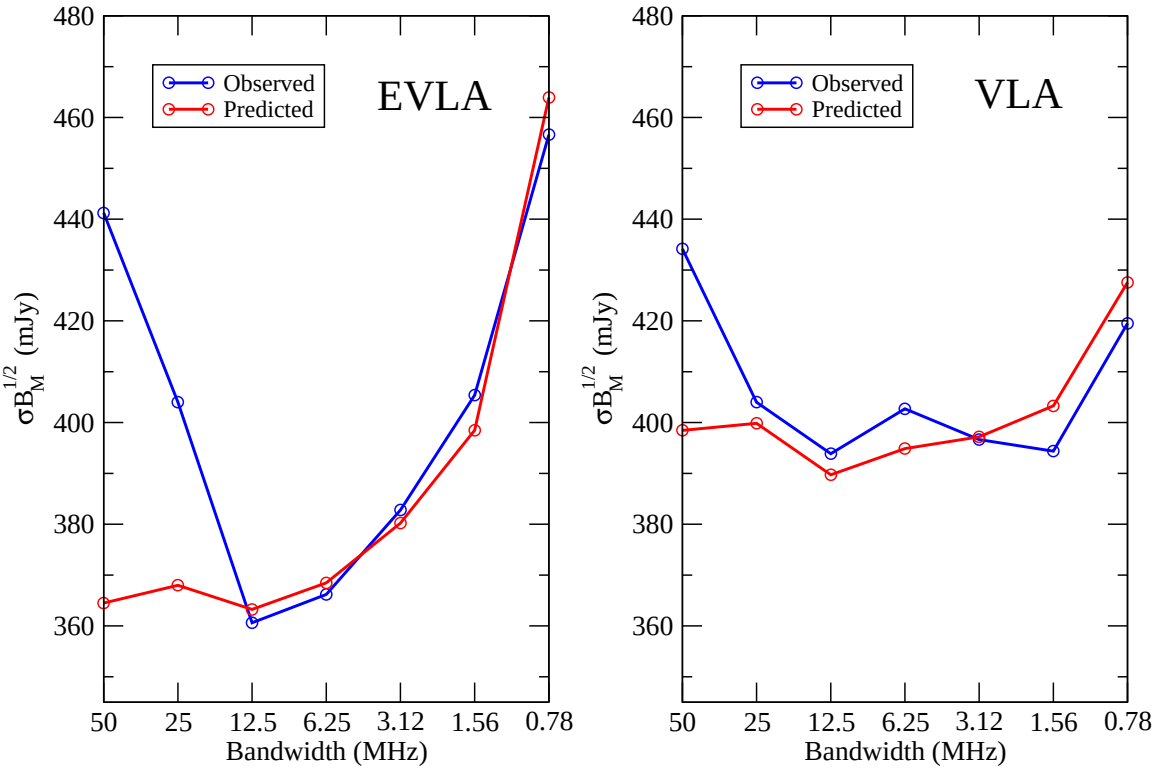

Figure 3: Showing the observed (blue) and predicted (red) sensitivities for the EVLA (left) and VLA (right), as a function of bandwidth, for observations made in the continuum mode. The sensitivies have been multiplied by $\sqrt{B_M}$, where B_M is the nominal bandwidth in MHz.

are 34 and 45 MHz for the EVLA and VLA respectively while at the nominal 50 MHz bandwidth, and is 21 MHz for the EVLA when at the nominal 25 MHz BW. The increase in T_{eff} seen in the narrower bandwidths for the EVLA due to aliased noise is well reflected in the sensitivity loss.

5.2 Spectral Line Results

The channel-dependent correlations provided when observing in the spectral line modes are not correlation coefficients – they are modified by the shape of the bandpass, and have been scaled such that the mean value over all channels is the same as that provided by the 'lag 0' value. If the bandpass were perfectly rectangular, with width equal to the full width of the nominal bandpass, then the individual correlator outputs would be the same as the continuum values, and would thus be correlation coefficients.

We can check that this scaling is done correctly by coherently summing the spectral data over the raw spectrum (that is, with no adjustment made for the bandpass), and determining if the antenna sensitivity parameter is the same. The result of this check shows that indeed the spectra are properly normalized for all spectral line data taken.

However, in general, the bandpasses are not rectangular, so the scaling operation will tend to raise the amplitude of the center channels, and depress those of the edge channels. The question of whether the central channels can be used to estimate antenna sensitivities is complicated by the fact that for some bandwidths, neither the bandpass, nor the SNR of the individual channels is uniform across the spectrum. For modest backend filter attenuation, the signal and the noise will be equally attenuated, so the SNR will not be affected. However, as the attenuation increases, the noise of the filter itself will become appreciable, so the edge channels will inevitably have a poorer SNR than the center. We should expect the central portions of the spectrum to have a better sensitivity than the overall continuum, but the degree to which this is true will depend on the spectral slope of the signal and the details of the bandpass.

Figure 4 shows the typical bandpasses for EVLA and VLA antennas. The bandpasses are in power units, normalized to their maximum. The VLA's 50 MHz baseband filters are far from rectangular, with a ∼3dB

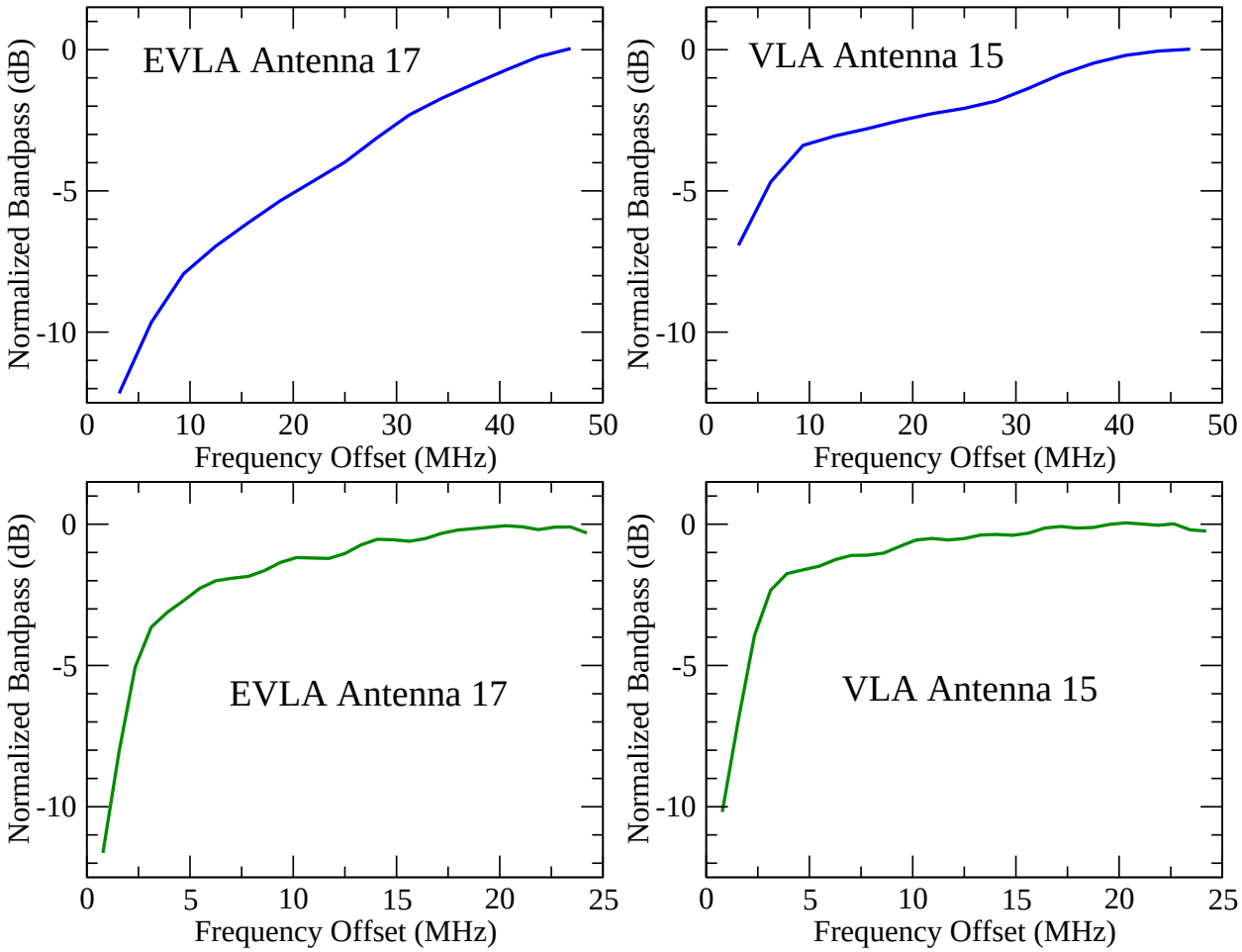

Figure 4: Typical bandpasses for EVLA antennas (left), and VLA antennas (right) at X-band. For this band, the baseband end is on the right. The upper panels show the 50 MHz-wide bandpasses, the lower panels the 25 MHz-wide bandpasses. Note that the EVLA antenna bandpass with 50 MHz baseband filter strongly attenuates the left side, resulting in a reduced sensitivity.

rolloff before the edge. The EVLA antennas all show a stronger roll-off – typically 8 dB before the filter edge – presumably due to the transition filter. The effective bandwidth for EVLA antennas at the nominal bandwidth of 50 MHz is about 35 MHz.

The variation in sensitivity across the bandpass can be easily measured through histograms of the noise for individual channels. The results of this are shown in Fig. 5 for the 50 and 25 MHz bandwidths. The VLA shows a modest roll-off in sensitivity across most of the bandpass, become severe only for the bottom 10 MHz, where the filter attenuation exceeds 5 dB. The slope in sensitivity is much greater for the EVLA antennas.

The noise increase at 50 MHz BW for the EVLA is more than expected from simple attenuation, and I suspect that most of the excess noise comes from the redistribution of sampler noise in the VLA's 3-level sampler. (See Carlson and Perley, EVLA Memo #83, and Thompson and Emerson, EVLA Memo #88).

The problems with bandpass attenuation and quantizer noise redistribution are absent for the narrow-band spectra, as shown in in Fig. 6, which shows the observed noise for the better EVLA and VLA antennas.

The strongly sloping passbands and variation of noise with channel seen at 50 and 25 MHz make analysis of the spectral line data problematical. The 6.25 MHz BW data are ideal for analysis, as the bandpasses are flat for both EVLA and VLA, and the sensitivity is uniform across the central 80% of the channels. I have thus utilized these data to compare the sensitivity predictions based on analysis of the correlation coefficients to the actual noise. The results of the analysis are shown in Table 2.

I first determined the on-sky sensitivities for various groups of antennas which have closely similar antenna sensitivities, as determined through analaysis of the corrrelation coefficients. The antennas involved are shown

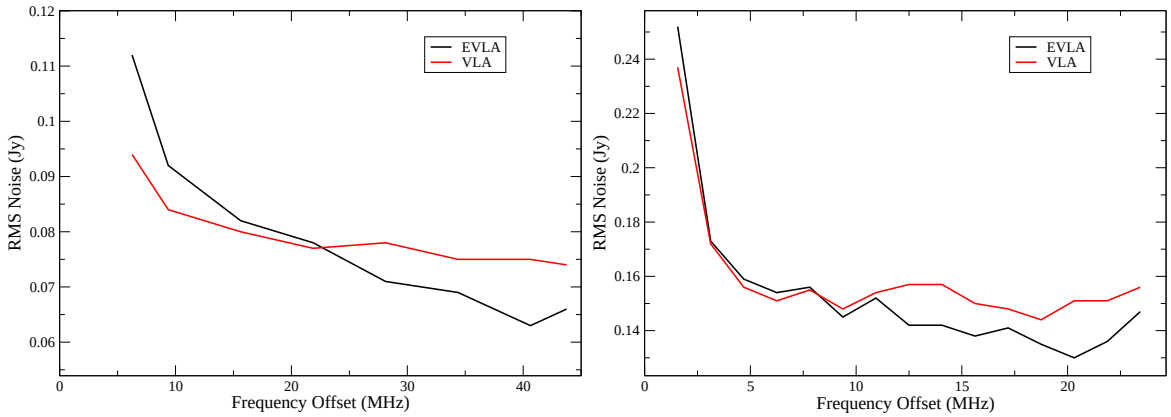

Figure 5: The variation in sensitivity across the spectrum for the 50 MHz-wide bandpass (left), and 25 MHz-wide bandpass (left). For both, Hanning smoothing has been applied to damp down ringing associated with the sharp cutoffs at the edges. The single-channel noise is a factor of 1.63 times larger than the values shown. Values shown are for a single baseline, with 0.417 seconds averaging.

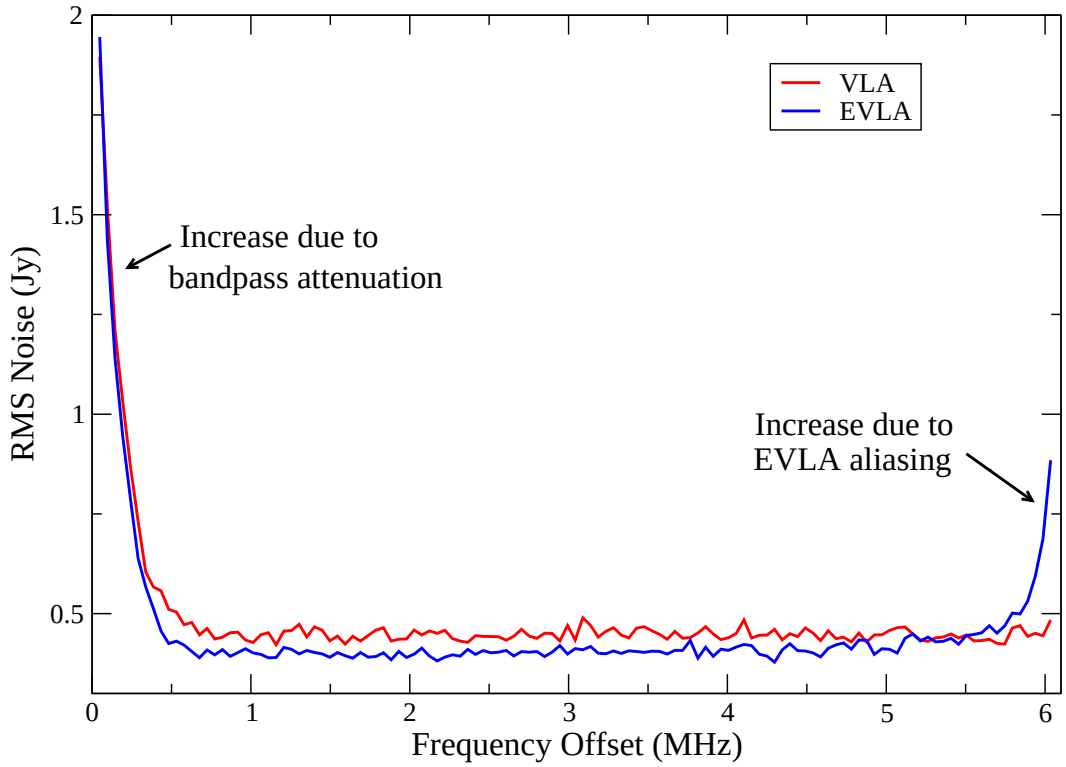

Figure 6: The variation in the sensitivity across the 6.25 MHz-wide spectrum. The sensitivity is very uniform across most of the bandpass. The rise on the low-frequency end is due to the back-end filter rolloff. On the high-frequency (baseband at X-band) end, the rise for the EVLA only is due to the aliasing in the transition filter. This is a transition problem only, and will not be present with the WIDAR correlator.

in columns 1 and 2. The on-sky sensitivites were found from the histograms of the real and imaginary parts of the visibilities, using channels 20 through 100. The statistical accuracy of the estimate is very high – there are typically 100,000 independent visibilities involved in each histogram. These values, in mJy, are shown in column 3. These on-sky sensitivities were then used to calculate the antenna sensitivities through use of equation 11,

Grouping	Antennas	σ	T_{es}	T_{ec}	T_{el}	T_{ec}/T_{es}	T_{el}/T_{es}	T_{ec}/T_{el}
		mJy	K	K	K			
Best 4 EVLA	5 13 16 26	606	48.5	50.0	42.9	1.03	0.88	1.16
Midd 6 EVLA	2 4 14 19 21 24	689	55.2	55.2	48.2	1.00	0.87	1.14
Next 4 EVLA	1 11 17 18	779	62.4	52.9	54.2	1.01	0.87	1.14
Best 2 VLA	15 27	653	52.3	50.5	45.6	0.97	0.87	1.11
Midd 4 VLA	6 7 8 20	721	57.7	57.8	53.4	1.00	0.93	1.08
Next 4 VLA	9 10 12 22	801	64.1	63.5	58.0	0.99	0.91	1.10

Table 2: The observed and predicted antenna sensitivies. Col. 1 and 2 show the antenna groups, Col. 3 gives the observed rms noise, in mJy. Col 4. gives the true antenna effective system temperature, using Eq. 11 with a channelwidth of 48.8 kHz, integration time of 3.33 seconds, and correlator efficiency of 0.79. Cols 5 and 6 give the estimated effective system temperatures derived from the correlation coefficients for the continuum, and spectral line, respectively. Col. 7 shows the ratio of the continuum-estimated line sensitivity to values observed – the values are very close to 1.0, indicating the estimates are excellent predictors. Col. 8 shows that the line-estimated sensitivities are too low, presumably due an offset from the normalization of the derived spectrum. Col. 9 is the ratio of the last two.

using an efficiency of 0.79. The results are shown in column 4. Column 5 shows the mean antenna sensitivity for the relevant group, as estimated from continuum correlation coefficients for the same bandwidth. Column 6 shows the antenna sensitivity, as estimated from the averaged central channels of the line data – these are expected to be too low, as the normalization process described earlier establishes a level based on the entire bandpass. The remaining columns show various ratios, which we describe next.

Column 7 in the table shows the ratio of the estimated sensitivity from the continuum correlation coefficients to that determined from direct observations in spectral line. The values are all very close to 1.0, incicating that the continuum-derived sensitivity parameters are an excellent predictor of spectral line sensitivity. Column 8 shows the ratio of the estimated sensitivity from the spectral line observations to those actually measured on blank sky. The ratios are all significantly less than 1.0, indicating that the spectral line 'correlation coefficients' are biased upwards by about 10% – presumably due to the normalization procedure. The final column is the ratio of the estimated sensitivities derived from continuum to that from the line, and shows the same offset.

In short, we can conclude that the estimates of antenna sensitivity through analysis of the correlation coefficients provided by the continuum system provide estimates accurate to typically 2% of the actual array sensitivity for both line and continuum modes, provided only that the appropriate effective bandwidths are utilized. This caveat effectively applies only to the 50 and 25 MHz bandwidths in continuum.